SIAM Review
Vol. 2, No. 3, July, 1960

NUMERICAL METHODS FOR REDUCING LINE AND SURFACE PROBE DATA[1]

O. H. Nestor[2] and H. N. Olsen[2]

Numerical methods are presented for integration of the inverted Abel integral equations encountered when using line or surface probes for measurement of radial distributions of physical properties of axially symmetric, inhomogeneous plasmas. In the case of radiation measurements the methods apply only where self-absorption is negligible. Numerical coefficients corresponding to a 30-zone division of the plasma radius have been tabulated. The methods have been applied to chosen analytical functions to show how inversion accuracy depends on the number of zones used and on the precision of the primary data.

INTRODUCTION

To determine the physical properties of an inhomogeneous, axially symmetric plasma one must obtain the true radial distribution of such quantities as radiation intensity, electrical current density, and heat transfer intensity. In high temperature plasmas where internal probes cannot be used, all observations must be made externally, and the data obtained then represents an integration of the true radial distribution over a finite extent of the plasma. Thus, all external probe data must be transformed to give the desired radial function.

Experimental probes may be classified as one of three types, i.e., point, line, or surface. The point probe, though it is most desirable in that it measures the radial function directly, is seldom practicable. An experimental problem encountered with both point and line probes is that of making dimensions of the probe small relative to the plasma diameter. In the case of radiation measurements where an "optical" line probe is used, magnification of the source can be employed such that the probe has an effective cross section which is negligibly small compared with plasma dimensions. The surface type probe is most applicable for determining quantities such as current density and heat transfer intensity at a point of the surface bounding the plasma.

Methods for obtaining radial distributions of quantities measured with a line probe have been described by several authors. In an application to spectral data, Finkelnburg and Maecker [1] calculate an average value of the radial function over an annular zone of the plasma cross section. The use of their method with a division of the cross section into N concentric zones involves first the evaluation of $N(N + 1)/2$ integrals which determine the elements of a triangular matrix. Inversion of this matrix then yields a set of numerical coefficients which may be used to transform the observed functions into corresponding radial functions. To our knowledge, the inverted matrix has not been published.

[1] Received by the editors.

[2] Linde Company, Division of Union Carbide Corporation.

Another approach yields the value of the radial function at specific points, not as an average over an annular zone, and avoids the tedious matrix inversion step. This approach involves an analytical inversion of the integral equation relating the measured probe function to the radial distribution function and solution of the resulting inverse equation. The latter must generally be done by numerical or graphical methods such as Hormann [2] and Gooderum and Wood [3] have described for the line probe case. The method presented in the following discussion is a simplification over those of Hormann and of Gooderum and Wood that is particularly significant when a large number of observed functions are to be inverted. In addition, the extension of numerical techniques to data obtained with plane surface probes is developed.

DISCUSSION

The mathematical basis of the techniques to be presented can be understood by reference to Figure 1(a). It is assumed that the system under study has an axis of symmetry normal to the plane of the paper at 0. The integral of the point function $f(r)$ (which is assumed to vanish for $r \geqq R$) over the shaded area ABC is given by

$$F(x) = 2 \int_x^R f(r) \cos^{-1} (x/r) r \, dr \tag{1}$$

and over the chord AC by

$$Q(x) = 2 \int_x^R \frac{f(r) r \, dr}{(r^2 - x^2)^{1/2}}. \tag{2}$$

$F(x)$ and $Q(x)$ represent quantities that can be measured directly by means of a "plane surface" probe and a "line" probe, respectively; except for algebraic

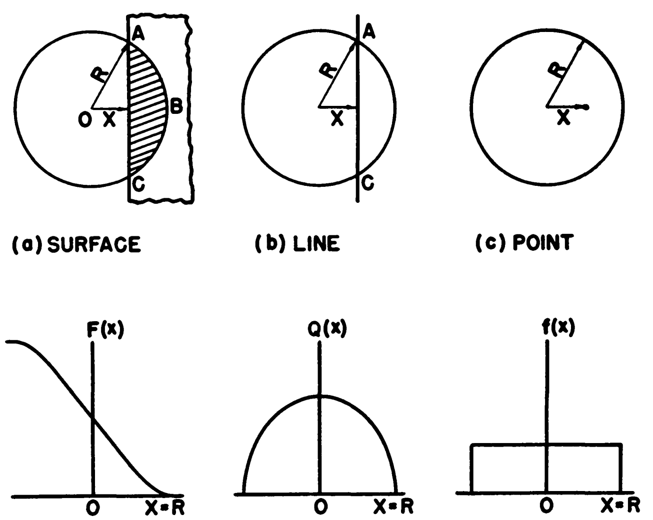

FIGURE 1. Probe types with functions each measures in a homogeneous, cylindrical source

sign, $Q(x)$ is seen to be just the derivative of $F(x)$. The form of each of the functions measured with the different probe types in a homogeneous cylindrical plasma is illustrated in Figure 1. Where both the line probe and surface probe are applicable, the former is preferred since, as will be shown later, a lower derivative of the observed function is used to determine the radial function. Hence, the distribution function derived from line probe data is not as sensitive to experimental errors as is that from surface probe data.

Equation (2) is recognized as the Abel integral equation whose solution is

$$f(r) = -\frac{1}{\pi}\int_r^R \frac{Q'(x)\,dx}{(x^2 - r^2)^{1/2}}. \tag{3}$$

Inasmuch as experimental functions are seldom expressed in integrable, analytical form, evaluation of the integral in Eq. (3) entails a numerical integration method.

1. INVERSION OF LINE PROBE DATA

In the numerical integration of Equation (3) as carried out by Gooderum and Wood the x-axis is divided into zones of equal width a, the nth zone being $x_n \leqq x < x_{n+1}$, $x_n = na$. By the transformation $r^2 = v$ and $x^2 = u$ Equation (3) becomes

$$f[r(v)] = -\frac{1}{\pi}\int_v^{R^2} \frac{Q'(u)\,du}{(u - v)^{1/2}}. \tag{4}$$

By dividing this integral into sub-integrals over each zone, assuming $Q(u)$ to be a linear function of u in each zone, the following form results:

$$f_k \equiv f(ak) = -\frac{1}{\pi}\sum_{n=k}^{N-1} Q_n'(u)\int_{(an)^2}^{[a(n+1)]^2} \frac{du}{[u - (ak)^2]^{1/2}} \tag{5}$$

where

$$Q_n'(u) = \frac{Q_{n+1}(u) - Q_n(u)}{a^2[(n+1)^2 - n^2]}.$$

After performing the indicated integration in Equation (5) and transforming back to the original coordinates, we get

$$f_k = -\frac{2}{\pi a}\sum_{n=k}^{N-1} A_{k,n}[Q_{n+1}(x) - Q_n(x)] \tag{6}$$

where

$$A_{k,n} = \frac{[(n+1)^2 - k^2]^{1/2} - [n^2 - k^2]^{1/2}}{2n+1}.$$

Gooderum and Wood have tabulated these coefficients for $N = 50$.

To avoid taking the differences $(Q_{n+1} - Q_n)$ in the experimental data, we have modified Eq. (6) as follows:

$$f_k = -\frac{2}{\pi a}\sum_{n=k}^{N} B_{k,n}Q_n \tag{6a}$$

where

$$B_{k,n} = -A_{k,k} \quad \text{for} \quad n = k$$

$$B_{k,n} = A_{k,n-1} - A_{k,n} \quad \text{for} \quad n \geqq k + 1.$$

The new set of coefficients may be obtained simply by taking successive differences of the tabulated $A_{k,n}$ coefficients.

2. INVERSION OF SURFACE PROBE DATA

Since the integrated function obtained with the line probe is the mathematical derivative, except for algebraic sign, of that obtained with the surface probe, one can determine the first derivative of the surface probe data numerically and then rely upon the line probe inversion in the form of Equation (6a). Alternatively, inversion of $F(x)$ to $f(r)$ can be made directly. Thus, using the same division of the x-axis the following definition is adopted for the first derivative within the nth zone:

$$F_n' = \frac{1}{2a}(F_{n+1} - F_{n-1}).$$

With this substitution for $-Q_n$ in Eq. (6a), that equation becomes

$$f_k = \frac{1}{\pi a^2} \sum_{n=k}^{N} B_{k,n}(F_{n+1} - F_{n-1}). \tag{7}$$

Again, as in the case of the line probe, it is desirable to eliminate the step of determining the differences $(F_{n+1} - F_{n-1})$. To this end the summation in Equation (7) is changed to

$$f_k = \frac{1}{\pi a^2} \sum_{n=k-1}^{N-1} C_{k,n} F_n \tag{7a}$$

where

$$C_{k,n} = -B_{k,k} \quad \text{for} \quad n = k - 1$$

$$C_{k,n} = -B_{k,k+1} \quad \text{for} \quad n = k$$

$$C_{k,n} = B_{k,n-1} - B_{k,n+1} \quad \text{for} \quad n \geqq k + 1.$$

These coefficients may be obtained by taking differences of the $B_{k,n}$ coefficients or second differences of the tabulated $A_{k,n}$ coefficients.

RESULTS AND CONCLUSIONS

The new $B_{k,n}$ and $C_{k,n}$ coefficients are listed in Tables I and II. The coefficients have actually been calculated for $N = 50$ but because of space limitations they are tabulated here only for the first 30 zones. If only m zones are required, the $m \times m$ triangular matrix of elements in the upper left corner may be used.

TABLE I. $B_{k,n}$ coefficients

n \ k	0	1	2	3	4	5	6	7	8	9	10	11	12	13	14
0	-1.000000														
1	+ .666667	-0.577350													
2	.133333	+ .358075	-0.447214												
3	.057143	.070053	+ .271781	-0.377965											
4	.031746	.035222	.051158	+ .227493	-0.333333										
5	.020202	.021536	.026613	.041731	+ .199503	-0.301511									
6	.013986	.014608	.016789	.021941	.035951	+ .179791	-0.277350								
7	.010256	.010586	.011689	.014024	.018970	.031985	+ .164953	-0.258199							
8	.007843	.008034	.008655	.009889	.012200	.016893	.029062	+ .153265	-0.242536						
9	.006192	.006310	.006687	.007407	.008662	.010898	.015346	.026799	+ .143752	-0.229416					
10	.005013	.005089	.005333	.005784	.006533	.007768	.009915	.014142	.024982	+ .135813	-0.218218				
11	.004141	.004193	.004356	.004655	.005133	.005882	.007085	.009145	.013174	.023486	+ .129058	-0.208514			
12	.003478	.003515	.003630	.003835	.004157	.004642	.005379	.006542	.008521	.012374	.022225	+ .123219	-0.200000		
13	.002963	.002990	.003072	.003218	.003443	.003774	.004256	.004976	.006100	.008003	.011700	.021145	+ .118107	-0.192450	
14	.002554	.002574	.002635	.002741	.002904	.003139	.003471	.003946	.004647	.005733	.007567	.011123	.020207	+ .113582	-0.185695
15	.002225	.002240	.002286	.002367	.002487	.002657	.002894	.003223	.003688	.004370	.005421	.007191	.010621	.019382	+ .109540
16	.001955	.001966	.002002	.002063	.002154	.002282	.002457	.002693	.003018	.003472	.004134	.005153	.006866	.010181	.018649
17	.001732	.001741	.001768	.001816	.001887	.001985	.002115	.002291	.002525	.002844	.003287	.003931	.004918	.006578	.009790
18	.001544	.001551	.001574	.001611	.001667	.001743	.001844	.001977	.002151	.002382	.002695	.003127	.003754	.004713	.006324
19	.001386	.001392	.001409	.001440	.001484	.001543	.001624	.001726	.001860	.002032	.002259	.002564	.002986	.003597	.004530
20	.001251	.001256	.001270	.001294	.001329	.001379	.001441	.001523	.001626	.001758	.001929	.002152	.002451	.002862	.003457
21	.001134	.001138	.001150	.001170	.001200	.001238	.001289	.001354	.001436	.001540	.001670	.001839	.002057	.002350	.002752
22	.001034	.001037	.001046	.001063	.001087	.001120	.001161	.001214	.001279	.001361	.001464	.001593	.001759	.001973	.002259
23	.000945	.000948	.000957	.000971	.000990	.001016	.001052	.001094	.001148	.001214	.001296	.001398	.001525	.001688	.001898
24	.000869	.000871	.000877	.000889	.000906	.000929	.000957	.000993	.001037	.001091	.001157	.001238	.001339	.001464	.001624
25	.000800	.000802	.000809	.000818	.000832	.000851	.000874	.000904	.000941	.000986	.001040	.001106	.001186	.001286	.001410
26	.000740	.000741	.000746	.000755	.000767	.000783	.000804	.000829	.000859	.000896	.000941	.000995	.001061	.001140	.001238
27	.000686	.000688	.000692	.000699	.000710	.000723	.000740	.000762	.000788	.000819	.000856	.000901	.000955	.001020	.001098
28	.000638	.000639	.000643	.000649	.000658	.000670	.000685	.000703	.000725	.000752	.000783	.000821	.000865	.000919	.000983
29	.000595	.000596	.000599	.000605	.000612	.000622	.000635	.000650	.000670	.000692	.000720	.000751	.000789	.000833	.000886

n \ k	15	16	17	18	19	20	21	22	23	24	25	26	27	28	29
15	-0.179605														
16	+ .105901	-0.174078													
17	.017993	+ .102602	-0.169031												
18	.009440	.017402	+ .099593	-0.164399											
19	.006095	.009124	.016864	+ .096834	-0.160128										
20	.004367	.005890	.008838	.016373	+ .094292	-0.156174									
21	.003331	.004218	.005703	.008577	.015923	+ .091941	-0.152499								
22	.002653	.003219	.004084	.005533	.008337	.015507	+ .089757	-0.149071							
23	.002178	.002563	.003116	.003961	.005376	.008116	.015122	+ .087721	-0.145865						
24	.001830	.002104	.002481	.003022	.003849	.005232	.007912	.014765	+ .085818	-0.142857					
25	.001567	.001769	.002038	.002407	.002936	.003746	.005099	.007721	.014431	+ .084033	-0.140028				
26	.001360	.001514	.001713	.001976	.002338	.002856	.003650	.004976	.007545	.014120	+ .082356	-0.137361			
27	.001195	.001315	.001466	.001661	.001920	.002275	.002783	.003560	.004860	.007379	.013827	+ .080776	-0.134840		
28	.001060	.001156	.001274	.001423	.001614	.001868	.002216	.002715	.003478	.004753	.007224	.013551	+ .079282	-0.132453	
29	.000950	.001026	.001120	.001236	.001382	.001571	.001819	.002161	.002651	.003399	.004652	.007078	.013292	+ .077868	-0.130189

TABLE II. $C_{k,n}$ coefficients

n/k	0	1	2	3	4	5	6	7	8	9	10	11	12	13	14
-1	+1.000000														
0	-0.666667	+0.577350													
1	-1.133333	-0.358075	+0.447214												
2	+0.609524	-0.647403	-0.271781	+0.377965											
3	.101587	+0.322853	-0.498372	-0.227493	+0.333333										
4	.036941	.048517	+0.245168	-0.419696	-0.199503	+0.301511									
5	.017760	.020614	.034369	+0.205552	-0.369284	-0.179791	+0.277350								
6	.009946	.010950	.014924	.027707	+0.180533	-0.333496	-0.164953	+0.258199							
7	.006143	.006574	.008134	.012052	.023751	+0.162898	-0.306412	-0.153265	+0.242536						
8	.004064	.004276	.005002	.006617	.010308	.021087	+0.149607	-0.284998	-0.143752	+0.229416					
9	.002830	.002945	.003322	.004105	.005667	.009125	.019147	+0.139123	-0.267518	-0.135813	+0.218218				
10	.002051	.002117	.002331	.002752	.003529	.005016	.008261	.017654	+0.130578	-0.252902	-0.129058	+0.208514			
11	.001535	.001574	.001703	.001949	.002376	.003126	.004536	.007600	.016461	+0.123439	-0.240443	-0.123219	+0.200000		
12	.001178	.001203	.001284	.001437	.001690	.002108	.002829	.004169	.007074	.015483	+0.117358	-0.229659	-0.118107	+0.192450	
13	.000924	.000941	.000995	.001094	.001253	.001503	.001908	.002596	.003874	.006641	.014658	+0.112096	-0.220207	-0.113582	+0.185695
14	.000738	.000750	.000786	.000851	.000956	.001117	.001362	.001753	.002412	.003633	.006279	.013954	+0.107486	-0.211832	-0.109540
15	.000599	.000608	.000633	.000678	.000750	.000857	.001014	.001253	.001629	.002261	.003433	.005970	.013341	+0.103401	-0.204344
16	.000493	.000499	.000518	.000551	.000600	.000672	.000779	.000932	.001163	.001526	.002134	.003260	.005703	.012804	+0.099750
17	.000411	.000415	.000428	.000452	.000487	.000539	.000613	.000716	.000867	.001090	.001439	.002026	.003112	.005468	.012325
18	.000346	.000349	.000359	.000376	.000403	.000442	.000491	.000565	.000665	.000812	.001028	.001367	.001932	.002981	.005260
19	.000293	.000295	.000304	.000317	.000338	.000364	.000403	.000454	.000525	.000624	.000766	.000975	.001303	.001851	.002867
20	.000252	.000254	.000259	.000270	.000284	.000305	.000335	.000372	.000424	.000492	.000589	.000725	.000929	.001247	.001778
21	.000217	.000219	.000224	.000231	.000242	.000259	.000280	.000309	.000347	.000397	.000465	.000559	.000692	.000889	.001198
22	.000189	.000190	.000193	.000199	.000210	.000222	.000237	.000260	.000288	.000326	.000374	.000441	.000532	.000662	.000854
23	.000165	.000166	.000169	.000174	.000181	.000191	.000204	.000221	.000242	.000270	.000307	.000355	.000420	.000509	.000635
24	.000145	.000146	.000148	.000153	.000158	.000165	.000178	.000190	.000207	.000228	.000256	.000292	.000339	.000402	.000488
25	.000129	.000130	.000131	.000134	.000139	.000146	.000153	.000164	.000178	.000195	.000216	.000243	.000278	.000324	.000386
26	.000114	.000114	.000117	.000119	.000122	.000128	.000134	.000142	.000153	.000167	.000184	.000205	.000231	.000266	.000312
27	.000102	.000102	.000103	.000106	.000109	.000113	.000119	.000126	.000134	.000144	.000158	.000174	.000196	.000221	.000255
28	.000091	.000092	.000093	.000094	.000098	.000101	.000105	.000112	.000118	.000127	.000136	.000150	.000166	.000187	.000212
29	.000082	.000082	.000084	.000085	.000087	.000090	.000094	.000098	.000105	.000112	.000120	.000131	.000143	.000160	.000179

n/k	15	16	17	18	19	20	21	22	23	24	25	26	27	28	29
14	+0.179605														
15	-0.105901	+0.174078													
16	-0.197598	-0.102602	+0.169031												
17	+0.096461	-0.191480	-0.099593	+0.164399											
18	.011898	+0.093478	-0.185895	-0.096834	+0.160128										
19	.005073	.011512	+0.090755	-0.180772	-0.094292	+0.156174									
20	.002764	.004906	.011161	+0.088257	-0.176051	-0.091941	+0.152499								
21	.001714	.002671	.004754	.010840	+0.085955	-0.171681	-0.089757	+0.149071							
22	.001153	.001655	.002587	.004616	.010547	+0.083825	-0.167621	-0.087721	+0.145865						
23	.000823	.001115	.001603	.002511	.004488	.010275	+0.081845	-0.163836	-0.085818	+0.142857					
24	.000611	.000794	.001078	.001554	.002440	.004370	.010023	+0.080000	-0.160296	-0.084033	+0.140028				
25	.000470	.000590	.000768	.001046	.001511	.002376	.004262	.009789	+0.078273	-0.156977	-0.082356	+0.137361			
26	.000372	.000454	.000572	.000746	.001016	.001471	.002316	.004161	.009571	+0.076654	-0.153855	-0.080776	+0.134840		
27	.000300	.000358	.000439	.000553	.000724	.000988	.001434	.002261	.004067	.009367	+0.075132	-0.150912	-0.079282	+0.132453	
28	.000245	.000289	.000346	.000425	.000538	.000704	.000964	.001399	.002209	.003980	.009175	+0.073698	-0.148132	-0.077868	+0.130189
29	.000204	.000237	.000280	.000336	.000412	.000523	.000685	.000939	.001367	.002161	.003897	.008994	+0.072341	-0.145500	-0.076528

To illustrate the "fit" afforded by the use of either set of coefficients we hav assumed a radial function of the form

$$\begin{aligned} f(r) &= 1 - 2r^2, & 0 \leqq r < \\ &= 2(1 - r)^2, & \tfrac{1}{2} \leqq r < \\ &= 0, & 1 \leqq \end{aligned}$$

implying $R = 1$. This function, qualitatively similar to the radial functions er

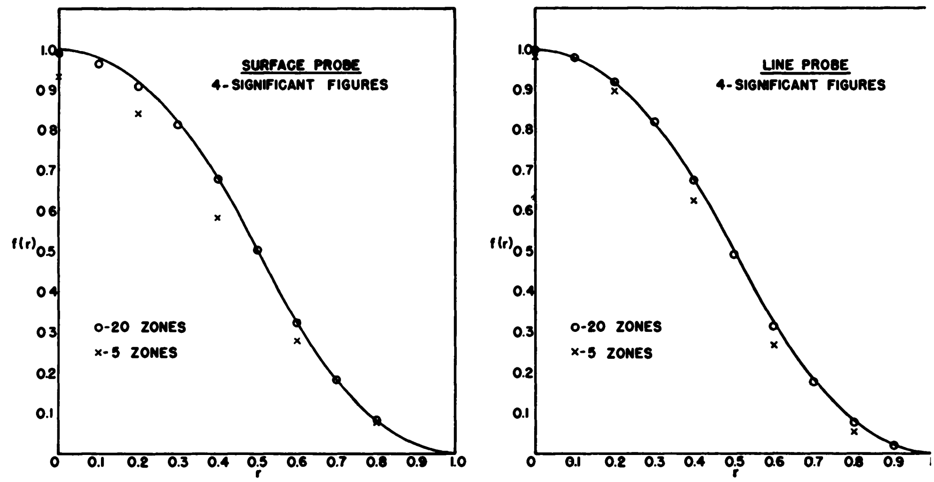

FIGURE 2. Effect of number of zones on the inversion

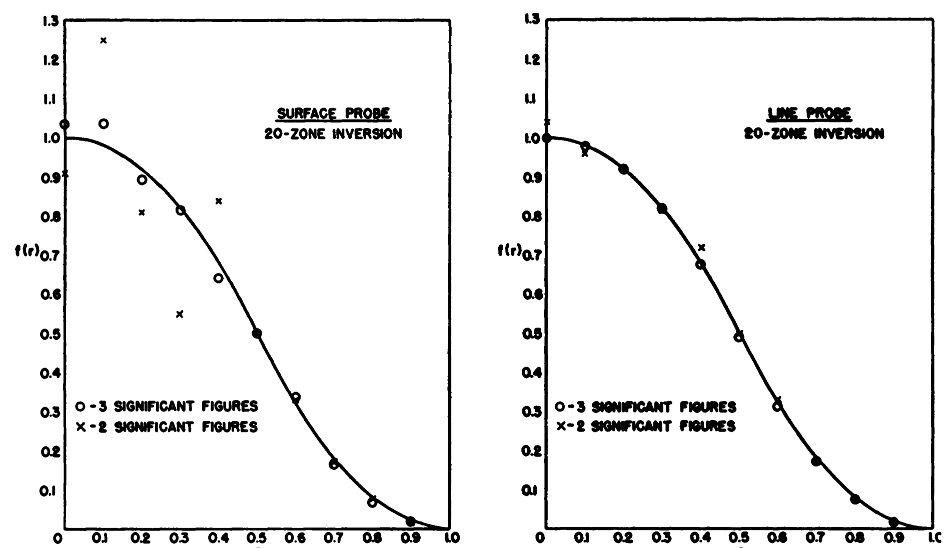

FIGURE 3. Effect of accuracy of primary data on the inversion

countered in plasma measurements, is plotted as the solid curve in Figures 2 and 3. The functions $F(x)$ and $Q(x)$ corresponding to the assumed $f(r)$ of Equation (8) were determined using Equations (1) and (2). The calculated values were then substituted in Equations (6a) and (7a), and the function $f(r)$ was redetermined.

The calculations were made to show how the calculated radial function varies with the number of zones assumed in the inversion process and with the accuracy of the initial data. The effect of the number of zones is illustrated in Figure 2 for assumed divisions into 5 and 20 zones using four significant figures. For the type of function assumed it is seen that the 20-zone inversions are quite satisfactory.

The effect of accuracy of experimental data is illustrated in Figure 3 for a 20-zone division of the x-axis. Errors in the radial function resulting from rounding the values of the integrated functions are considerably greater for the surface probe than for the line probe method. This is a direct result of the fact that second differences of the integrated function are involved in the surface probe inversion.

REFERENCES

1. W. Finkelnburg and H. Maecker, *Handbuch der Physik, Band XXII, Gasentladungen II*, Springer-Verlag, Berlin, 1956.
2. H. Hormann, Zeit. f. Physik, 97, (1935), 539–560.
3. P. B. Gooderum and G. P. Wood, NACA Technical Note 2173 (August 1950).